Calculation of the thermal conductivity of $L_2SrAl_2O_7$ (L = La, Nd, Sm, Eu, Gd, Dy)

Jing Feng,[1,2] Chunlei Wan,[1] Bing Xiao,[3] Rong Zhou,[2] Wei Pan,[1,*] and David R. Clarke[4]

[1]*State Key Laboratory of New Ceramics and Fine Processing, Department of Materials Science and Engineering, Tsinghua University, Beijing 100084, P. R. China*

[2]*Key Laboratory of Advanced Materials of Precious-Nonferrous Metals, Education Ministry of China, Kunming University of Science and Technology, Kunming 650093, P. R. China*

[3]*Department of Physics, School of Science and Engineering, Tulane University, LA 70118, USA*

[4]*School of Engineering and Applied Science, Harvard University, Cambridge, MA 02138, USA*

(Received 5 January 2011; revised manuscript received 23 April 2011; published 12 July 2011)

Density functional perturbation theory, combined with quasi-harmonic approximation theory and the Debye theory, has been used to calculate the thermal conductivity of the double-perovskite perovskite slab–rocksalt layer oxide compounds $L_2SrAl_2O_7$ (L = La, Nd, Sm, Eu, Gd, and Dy), a promising class of high-temperature thermal insulators. The predicted properties are compared with experimental data and show excellent agreement from room temperature up to 1000 °C. This indicates that the methodology is an effective approach to calculating the thermal conductivity of complex, defect-free crystal structures.

DOI: 10.1103/PhysRevB.84.024302 PACS number(s): 65.40.Ba, 62.20.de, 71.15.Mb

I. INTRODUCTION

Materials with low thermal conductivity at high temperatures are required for a variety of applications, the most notable being as thermal barrier coatings for providing thermal insulation to alloy blades and vanes in gas turbine engines and diesel engines.[1,2] In the most demanding of these turbine applications, the current coating material of choice, 6–8 wt.% yttria-stabilized zirconia (8YSZ), enables the turbine gas temperatures to exceed to melting temperatures of the alloy components they protect.[3,4] For increased energy efficiency, new low thermal conductivity materials will probably be needed for next-generation engines, and there is currently a search for oxides with still lower thermal conductivity.[5–7] As is well known, low thermal conductivity can be achieved by introducing porosity, but pores are unstable at very high temperatures; therefore, the search is for oxides with low intrinsic thermal conductivity. As part of this search, the rare-earth strontium aluminates ($L_2SrAl_2O_7$, L = La, Nd, Sm, Eu, Gd, and Dy) have been identified as candidate materials for further study. These compounds, which are analogous in structure to the rare-earth manganites, consist of periodic stacking of double-perovskite blocks, formed from AlO6 octahedra, alternating with rocksalt blocks, as illustrated in Fig. 1. Its space group is *I4/mmm* (No. 139), with the rare-earth and Sr^{2+} ions occupying the 4e (0, 0, 0.318) and 2b (0, 0, 0.5) Wyckoff sites, the Al^{3+} cation occupying the 4e (0, 0, 0.0941) sites, and the O^{2-} anion occupying the 2a (0, 0, 1), 8g (0, 0.5, 0.097), and 4e (0, 0, 0.1991) sites. The reported lattice parameters for each of the compounds determined by x-ray diffraction are listed in Table I.

Although there are general guidelines for identifying compounds that can be expected to have low thermal conductivity based on having a high average atomic weight, a large number of atoms per unit cell, ions on several sublattices, loose bonding, and highly disordered and distorted structures,[8,9] the ability to calculate the thermal conductivity and its temperature dependence of complex structures, such as the rare-earth strontium aluminates, without molecular dynamics or first-principles computation is lacking. This is partly because the number of phonon modes increases with structural complexity and the number of atoms per unit cell.

II. COMPUTATIONAL APPROACH

In this paper, we use density functional perturbation theory (DFPT),[10] combined with quasi-harmonic approximation (QHA),[11] to compute the parameters used in the Debye model to calculate the thermal conductivity as a function of temperature. DFPT, which is a combination of the standard density functional theory with a linear electron density response, is used for these calculations to reduce the computational cost of determining the phonon frequencies throughout the Brillouin zone. By combining the method with QHA, we follow the approach used by a number of researchers who have successfully predicted many of the thermal properties (but not the thermal conductivity) of compounds, including Al,[12] Ag,[13] Cu,[14] AlLi,[15] and NiAl and PdTe,[16] but these are all much simpler compounds than the rare-earth strontium aluminates considered in this paper. From the calculated phonon modes and the free energy functions, we evaluate the thermal conductivity using the standard Debye expression (1)[17]:

$$\kappa(T) = \frac{v_m}{3}\int_0^{\omega_{\max}} C_v(\omega,T)\, l(\omega,T)\, d\omega \qquad (1)$$

$C_v(\omega)$ is the spectral contribution to heat capacity at constant volume per unit volume, v_m is the average sound velocity, and $l(\omega,T)$ is the intrinsic phonon mean free path at different frequencies. This is an approximate expression, because as described later, the average phonon velocities are obtained from the computed bulk and shear moduli by polycrystalline averaging and thus are taken out of the integral. Also, the value of $\omega_{\max}$ was calculated from the computed Debye temperature and thus is an isotropic value. Despite these approximations, the combination of DFPT, QHA, and the Debye equation enables us to calculate the phonon modes for single crystals, calculate their elastic constants, and then compute the polycrystalline averages for comparison with

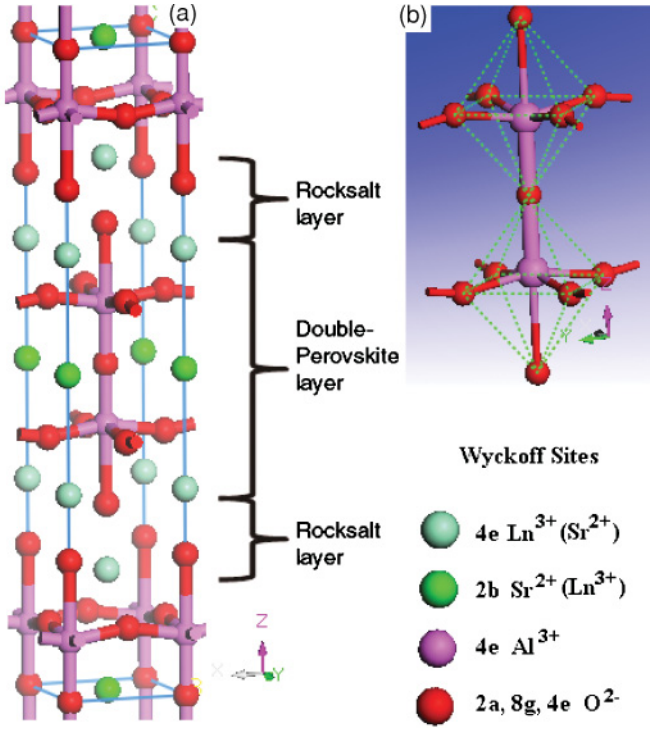

FIG. 1. (Color online) Crystal structure of the double-perovskite slab–rocksalt layer $L_2SrAl_2O_7$ (L = La, Nd, Sm, Eu, Gd, and Dy) compound. (a) A unit cell indicating the perovskite and rocksalt layers. (b) The basic AlO_6 octahedra of the structure. The Wyckoff sites of atoms in the crystal are listed in the figure.

the experimental data obtained for polycrystalline materials.[18] (Single crystals of these highly refractory compounds have not been grown, so single crystal data is unavailable for comparison.) The methodology is consequently different from more direct methods such as molecular dynamics simulations and frozen-phonon calculations (in which the unit cell must be large enough to match the wavelength of the phonon mode)[19–21] but enables us to compute physical properties, such as elastic moduli, as well as the polycrystalline thermal conductivity.

The first-principles calculations based on DFPT were performed using the Cambridge Serial Total Energy Package code.[22] Ultrasoft pseudopotentials were employed to represent the interactions between the ionic cores and the valence electrons. The exchange correction energies for the generalized gradient approximation were evaluated using the Perdew-Burke-Ernzerhof scheme.[23–25] A special **k** point sampling method was used for the integration by setting as $10\times10\times12$ for each of the rare-earth compounds, with a Monkhorst-Pack scheme in the first irreducible Brillouin zone. The calculations were continued until the average forces acting on each of the ions became smaller than 1.0×10^{-6} eV/atom. The specific valence electrons included in the calculation were as follows: for O atoms, O $2s^2\ 2p^4$; for Al atoms, $3s^2\ 3p^1$; for Sr atoms, $4s^2\ 4p^6\ 5s^2$; for La atoms, $5s^2\ 5p^6\ 5d^1\ 6s^2$; for Nd atoms, $4f^4\ 5s^2\ 5p^6\ 6s^2$; for Sm atoms, $4f^6\ 5s^2\ 5p^6\ 6s^2$; for Eu atoms, $4f^7\ 5s^2\ 5p^6\ 6s^2$; for Gd atoms, $4f^7\ 5s^2\ 5p^6\ 5d^1\ 6s^2$; and for Dy atoms, $4f^{10}\ 5s^2\ 5p^6\ 6s^2$. The maximum energy cutoff value for the plane wave expansions was 500.0 eV. The unit cell dimensions calculated are listed in Table I and compared with the dimensions reported by Zvereva *et al.*[26] The calculations generally overestimate the unit cell dimensions and volumes. Consequently, the calculated densities are somewhat lower than those measured.

In QHA theory, the Helmholtz free energy at a given volume V and temperature T can be expressed in terms of the phonon frequencies determined from the DFPT computations using[12,27,28]

$$F_{\rm vib}(V,T) = \frac{1}{2}\sum_{n,\mathbf{q}}\hbar\omega(n,\mathbf{q}) + k_BT\sum_{n,\mathbf{q}}\ln\left(1-e^{-\hbar\omega(n,\mathbf{q})/(k_BT)}\right), \quad (2)$$

where the frequency of the nth mode, $\omega(n,\mathbf{q})$, depends on the unit cell volume and the masses of the constituent atoms. In turn, the intrinsic phonon mean free path $l(\omega,T)$ was calculated using the relationship[12,27]

$$1/l(\omega,T) = 2\gamma\,(n,\mathbf{q})^2\,(kT/Ga^3)\,(\omega\,(n,\mathbf{q})^2/v_s\omega m), \quad (3)$$

where γ is a Gruneisen anharmonicity parameter, a^3 is the volume per atom, and ω_m is the Debye frequency of the acoustic branches. To obtain a simple expression for the temperature dependence of the unit cell volume, we express the Gruneisen parameter[12,28] of mode $n,\mathbf{q}$ as

$$\gamma(n,\mathbf{q}) = -\frac{V}{\omega(n,\mathbf{q})}\frac{\partial\omega(n,\mathbf{q})}{\partial V}. \quad (4)$$

We also assume that the phonon frequencies over the range of the temperature we are interested in can be well approximated by a Taylor expansion up to the second order of volume[12,28]:

$$\omega(n,\mathbf{q}) = \omega_0(n,\mathbf{q})\cdot\left[1-\gamma_0(n,\mathbf{q})\cdot\left(\frac{V-V_0}{V_0}\right) - \frac{1}{2}\beta_0(n,\mathbf{q})\cdot\left(\frac{V-V_0}{V_0}\right)^2\right] \quad (5)$$

$$\beta(n,\mathbf{q}) \equiv -\frac{V^2}{\omega(n,\mathbf{q})}\frac{\partial^2\omega(n,\mathbf{q})}{\partial V^2} \quad (6)$$

Here, the concavity parameter β is proportional to the second derivative of the phonon frequencies and describes the deviation from the linear behavior of the volume dependence of the frequency $\omega(n,\mathbf{q})$. As temperature increases, the unit cell volume of the material expands and the strength of chemical bond weakens, so the elastic constants decrease with the temperature. In QHA, we made a careful study of the temperature effect for the modulus calculated from the phonon frequencies so as to obtain accurate values of the average sound velocity at high temperatures. The isothermal bulk modulus $B_T \equiv V(\partial^2F/\partial V^2)|_T$ is given by[12,27,28]

$$B_T = V\frac{\partial^2Uo}{\partial^2V^2} - \frac{1}{2V}\sum_{n,\mathbf{q}}\frac{\hbar\omega(n,\mathbf{q})}{\cosh\cdot\frac{\hbar\omega(n,\mathbf{q})}{k_BT}-1} \times\left[\frac{\hbar\omega(n,\mathbf{q})}{k_BT}\cdot\gamma^2(n,\mathbf{q}) + \beta(n,\mathbf{q})\cdot\sinh\frac{\hbar\omega(n,\mathbf{q})}{k_BT}\right]. \quad (7)$$

TABLE I. Lattice parameters, Debye temperature, sound velocity, and mechanical properties of $L_2SrAl_2O_7$ (L = La, Nd, Sm, Eu, Gd, and Dy).

	$La_2SrAl_2O_7$		$Nd_2SrAl_2O_7$		$Sm_2SrAl_2O_7$		$Eu_2SrAl_2O_7$		$Gd_2SrAl_2O_7$		$Dy_2SrAl_2O_7$	
Method	cal.	exp.	cal.	exp.	cal.	exp.	cal.	exp.	cal.	exp.	cal.	exp.
L^{3+} (nm)	0.122	0.116	0.113	0.112	0.111	0.108						
a (nm)	0.378	0.377	0.376	0.372	0.373	0.372	0.373	0.371	0.371	0.371	0.373	0.371
c (nm)	2.048	2.02	2.009	1.994	2.008	1.988	1.998	1.983	1.980	1.978	1.961	1.957
c/a	5.418	5.358	5.343	5.354	5.383	5.344	5.357	5.345	5.337	5.332	5.257	5.275
V (nm^3)	0.293	0.287	0.284	0.278	0.279	0.274	0.278	0.273	0.273	0.272	0.273	0.269
ρ (g/m^3)	5.879	6.127	6.331	6.493	6.583	6.697	6.655	6.76	6.936	6.936	7.006	7.155
B (GPa)	178	137	179	140	174	160	171	160	189	175	184	188
E (GPa)	161	166	218	186	251	252	224	240	269	258	246	230
G (GPa)	99	100	106	104	106	109	106	102	110	109	109	109
B/G	1.803	1.347	1.685	1.346	1.638	1.465	1.617	1.569	1.722	1.602	1.695	1.725
v	0.197	0.203	0.19	0.199	0.21	0.223	0.213	0.237	0.217	0.243	0.227	0.257
Θ_D (K)	583	586	593	590	584	598	581	576	584	590	577	585
v_m (m/ s)	4562	4623	4555	4631	4455	4687	4427	4499	4415	4596	4375	4547

At $T = 0$ K, the second term in the square brackets of Eq. (7) gives the zero-point energy contribution to the bulk modulus.

III. RESULTS AND DISCUSSION

The calculated bulk moduli obtained this way are shown in Fig. 2 and listed in Table I. Similar results were obtained using the full-electron method (Demol[3] software) for the lattice parameters, elastic constants, and bulk modulus of $La_2SrAl_2O_7$. The calculated bulk modulus of all compounds varies between 140 and 188 GPa, which is typical for most oxides with strong ionic and polarized covalent bonds.

For comparison with the experimental data obtained with polycrystalline material, the shear moduli G, Young's moduli E, and Poisson ratios were calculated from the computed single crystal elastic constants using the Voigt-Ruess-Hill method. The values of these polycrystalline properties are listed in Table I and shown in Fig. 2. The calculated Poisson ratios (v) are similar to those measured and are typical of many oxides. The average sound velocity v_m is calculated from the longitudinal wave speeds v_p and transverse wave speeds v_s,[29] determined from the isothermal bulk and shear moduli, respectively, computed using Eq. (7):

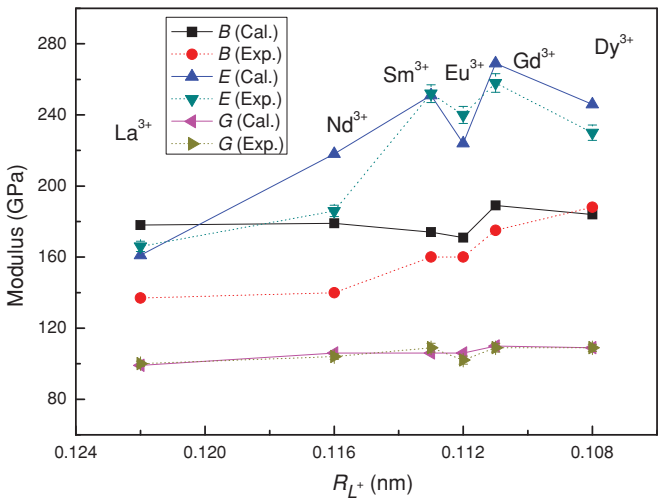

FIG. 2. (Color online) Bulk modulus (B), Young's modulus (E), and shear modulus (G) of $L_2SrAl_2O_7$ (L = La, Nd, Sm, Eu, Gd, and Dy). The full lines join the calculated values, and the dashed lines join the experimental data in this paper. The measurement errors are commensurate with the size of the data points.

$$v_m = \left[\frac{1}{3}\left(\frac{2}{v_s^3} + \frac{1}{v_p^3}\right)\right]^{-\frac{1}{3}} \tag{8}$$

$$\begin{cases} v_p = \sqrt{\left(B + \frac{4}{3}G\right)/\rho} \\ v_s = \sqrt{G/\rho} \end{cases} \tag{9}$$

The remaining parameter required for evaluating the thermal conductivity using Eq. (7) is the heat capacity. In the Debye model, this is given by[12,20]

$$c_v^D(T) = 9Nk_B\left(\frac{T}{\Theta_D}\right)^3 \int_0^{\Theta_D/T} \frac{x^4 e^x}{(e^x - 1)^2} dx \tag{10}$$

where, Θ_D is the Debye temperature. Similarly, the Debye temperature can be expressed as

$$\Theta_D = \frac{h}{k_B}\left[\frac{3n}{4\pi}\left(\frac{N_A\rho}{M}\right)\right]^{1/3} v_m \tag{11}$$

N_A is Avogadro's number, n is the number of atoms in the formula unit, M is the molecular weight of the formula unit, and ρ is the density computed from first principles. The Debye temperatures calculated this way and using the computed densities are listed in Table I. In the table, they are compared with those obtained from calculations based on averaging the sound velocities in the crystal measured using ultrasonic resonance methods.[30]

Figure 3 shows a comparison among heat capacities determined from our calculations, obtained using the Neumann-Kopp (N-K) rule and those measured. The N-K method

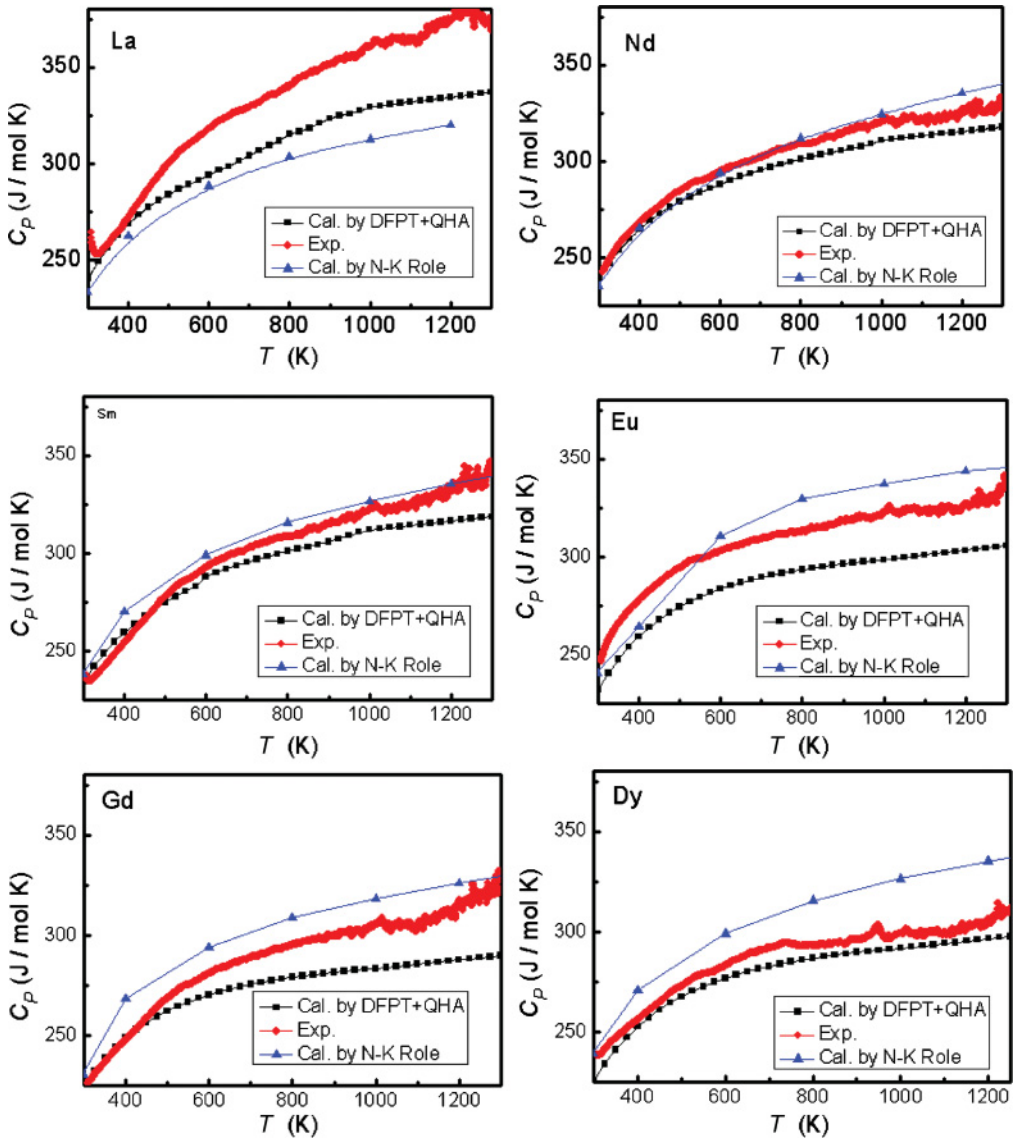

FIG. 3. (Color online) Heat capacities of $L_2SrAl_2O_7$ (L = La, Nd, Sm, Eu, Gd, and Dy). For comparison, the calculations using the N-K method (blue triangles) and those computed using QHA (black squares) are plotted with the experimental values (the red lines).

calculates the heat capacity of a compound from the compositionally weighted heat capacities of the constituent oxides (SrO, L_2O_3, and Al_2O_3).[31] With the exception of $La_2SrAl_2O_7$, the values obtained by the N-K rule are consistently larger than the calculated and experimental values. Over the temperature range 298–600 K, the heat capacities calculated by DFPT combined with the QHA method are consistent with the experimental values. However, at higher temperatures, the calculated heat capacities are underestimates. This would be consistent with the heat capacity calculated using QHA only including the vibrational entropy. One contribution not included in QHA is any configurational entropy associated with antisite defects. These arise because an unusual feature of the compounds is that the Sr^{2+} and L^{3+} ions are distributed between the two sites, one in the rocksalt block (A_2) and the other in the perovskite block. From the x-ray data, the concentration of the L^{3+} occupying the A_2 site in the rocksalt layer increases as the atomic number of the L^{3+} ion is increased from La^{3+} to Dy^{3+}.[26] Consequently, the contribution from the configurational entropy of the antisite defect could play a role in determining the heat capacity at higher temperatures.

The thermal conductivities of the six rare-earth strontium aluminate compounds calculated from the Debye equation using the values of the individual parameters, obtained using the methodology described earlier, are plotted as a function of temperature in Fig. 4. There they are compared with the measurements reported in the literature. As can be seen from Fig. 4, the values are in good agreement in terms of both their absolute values and their temperature dependence with those reported.[21] Even the values for the $Dy_2SrAl_2O_7$ compound differ by $<15\%$ from those measured. Interestingly, where there is a difference, the calculated values are systematically somewhat larger. Although this could be because of the presence of antisite defects mentioned earlier, the calculated and measured values are so close for the Nd, Sm, and Eu

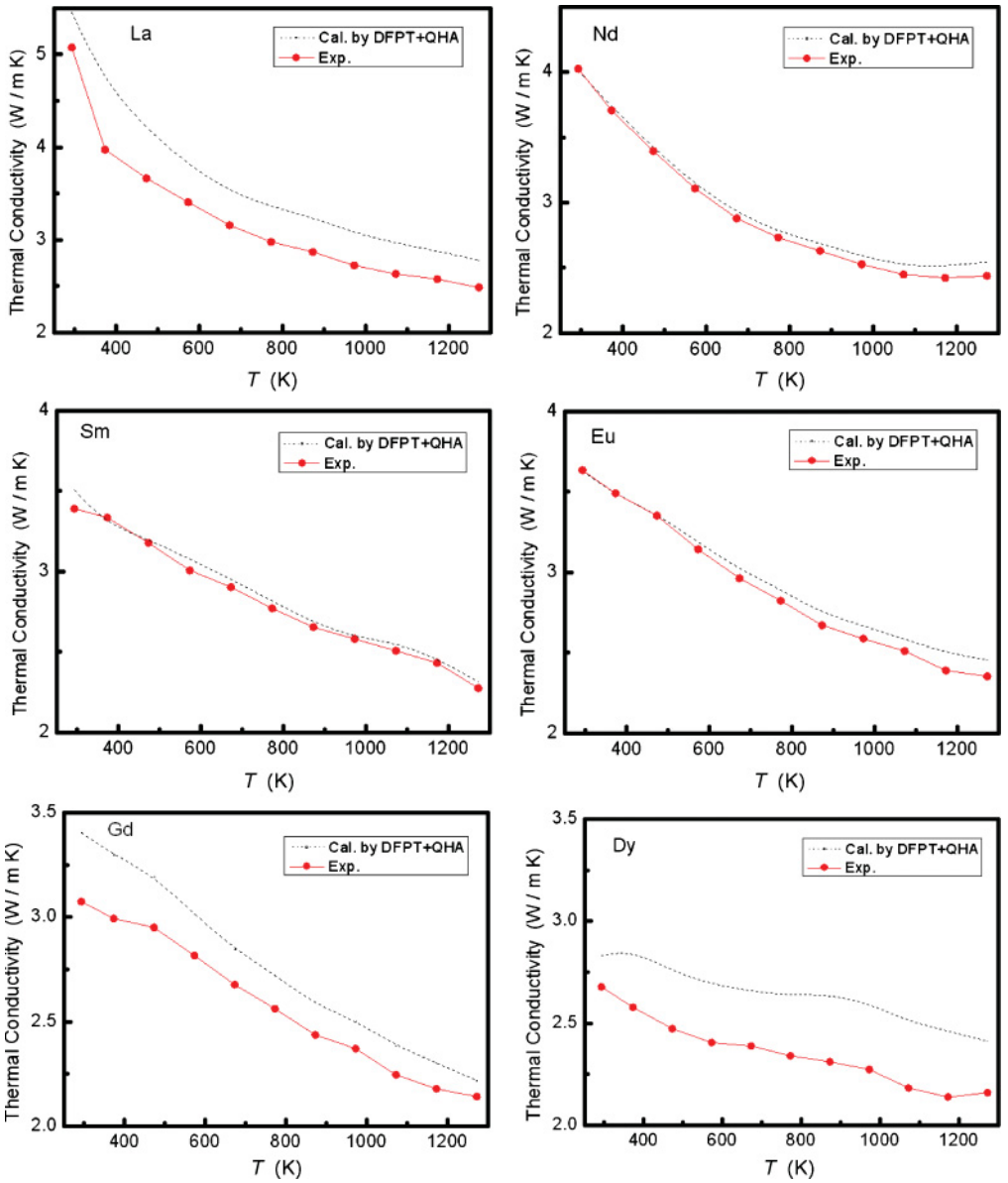

FIG. 4. (Color online) Thermal conductivities of $L_2SrAl_2O_7$ (L = La, Nd, Sm, Eu, Gd, and Dy) as a function of temperature. The red lines are the experimental measurements, and the dashed lines are the values calculated in this paper.

compounds that they suggest the discrepancy is more likely because of small measurement uncertainties, in particular errors in measuring the densities. In general, it is expected that the larger the bulk modulus, the higher the Debye temperature of the compound.[30] Based on this consideration alone, we would expect from the Debye expression for conductivity that the $Dy_2SrAl_2O_7$ should have a lower thermal conductivity than other compounds, as indeed is found experimentally.

IV. CONCLUSION

In summary, the application of DFPT, combined with QHA theory and the Debye model, has been used to compute the thermal conductivity of a series of rare-earth strontium aluminate-layered compounds from room temperature up to 1000 °C. The predicted conductivities for the polycrystalline samples are in good agreement with those previously measured over the entire range of temperatures, from room temperature up to 1000 °C. This suggests that the methodology described here is an effective way to calculate the thermal conductivities of a variety of complex oxides. The one shortcoming is that the methodology is currently limited to defect-free oxides, because defects are not specifically taken into account.

ACKNOWLEDGMENT

The authors are grateful to the National Natural Science Foundation of China (Grants No. 50232020 and No. 50572042) for financial support. The collaboration with Harvard University has been supported by the U.S. National Science Foundation through World Materials Network Grant No. DMR-0710523.

*panw@mail.tsinghua.edu.cn

[1] N. P. Padture, M. Gell, and E. H. Jordan, Science **296**, 280 (2002).
[2] K. E. Sickafus, L. Minervini, R. W. Grimes, J. A. Valdez, M. Ishimaru, and F. Li, Science **289**, 748 (2000).
[3] J. A. Thompson and T. W. Clyne, Acta. Mater. **49**, 1565 (2001).
[4] H. Lehmann, D. Pitzer, G. Pracht, R. Vassen, and D. Stvoer, J. Am. Ceram. Soc. **86**, 1338 (2003).
[5] J. R. Nicholls, K. J. Lawson, A. Johnstone, and D. S. Rickerby, Surf. Coat. Tech. **151-152**, 383 (2002).
[6] X. Q. Cao, R. Vassen, and W. Fishcher, Adv. Mater. **15**, 1438 (2003).
[7] D. R. Clarke, Surf. Coat. Technol. **163**, 67 (2003).
[8] D. R. Clarke and C. G. Levi. Ann. Rev. Mater. Res. **33**, 383 (2003).
[9] D. R. Clarke and S. R. Phillpot, Mater. Today **8**, 22 (2005).
[10] S. Baroni, S. de Gironcoli, A. D. Corso, and P. Giannozzi, Rev. Mod. Phys. **73**, 515 (2001).
[11] S. Baroni, P. Giannozzi, and E. Isaev, Rev. Mineral. Geochem., doi:10.2138:rmg.2009.71.3 (2010).
[12] A. A. Quong and A. Y. Liu, Phys. Rev. B **56**, 7767 (1997).
[13] J. Xie, S. de Gironcoli, S. Baroni, and M. Scheffler, Phys. Rev. B **59**, 965 (1999).
[14] S. Narasimhan and S. de Gironcoli, Phys. Rev. B **65**, 064302 (2002).
[15] M. H. F. Sluiter, M. Weinert, and Y. Kawazoe, Phys. Rev. B **59**, 4100 (1999).
[16] G. J. Ackland, X. Y. Huang, and K. M. Rabe, Phys. Rev. B **68**, 214104 (2003).
[17] G. Grimvall, *Thermophysical Properties of Materials, North Holland* (Elsevier BV, Amsterdam, 1999).
[18] C. Wan, T. D. Sparks, W. Pan, and D. R. Clarke, J. Am. Ceram. Soc., **93**, 1457 (2010).
[19] D. A. Broido and T. L. Reinecke, Phys. Rev. B **70**, 081310(R) (2004).
[20] D. A. Broido, M. Malorny, G. Birner, N. Mingo, and D. A. Stewart, Appl. Phys. Lett. **91**, 231922 (2007).
[21] A. Ward, D. A. Broido, D. A. Stewart, and G. Deinzer, Phys. Rev. B **80**, 125203 (2009).
[22] M. D. Segall, P. J. D. Lindan, M. J. Probert, C. J. Pickard, P. J. Hasnip, S. J. Clark, and M. C. Payne, J. Phys. Condens. Matter **14**, 2717 (2002).
[23] P. Hohenberg and W. Kohn, Phys. Rev. **136**, B864 (1964).
[24] G. Kresse and D. Joubert, Phys. Rev. B **59**, 1758 (1999).
[25] J. P. Perdew, K. Burke, and M. Ernzerhof, Phys. Rev. Lett. **77**, 3865 (1996).
[26] I. Zvereva, Y. Smirnov, V. Gusarov, V. Popova, and J. Choisnet, Solid State Sci. **5**, 343 (2003).
[27] P. G. Klemens, Phys. B **263-264**, 102 (1999).
[28] A. Debernardi, M. Alouani, and H. Dreysse, Phys. Rev. B **63**, 064305 (2001).
[29] B. Liu, J. Y. Wang, Y. C. Zhou, T. Liao, and F. Z. Li, Acta Mater. **58**, 4369 (2010).
[30] C. Kittel, *Introduction to Solid State Physics* (John Wiley & Sons, Inc., New York, 1997).
[31] Y. J. Liang, Y. C. Che, and X. X. Liu, *Manual of Practical Inorganic Matter Thermodynamics* (Northeastern University Press, Shenyang, P. R. China, 1993).